UNICAMP

SBU
SISTEMA DE BIBLIOTECAS DA UNICAMP

UNIVERSIDADE ESTADUAL DE CAMPINAS
SISTEMA DE BIBLIOTECAS DA UNICAMP
REPOSITÓRIO DA PRODUÇÃO CIENTIFICA E INTELECTUAL DA UNICAMP

Versão do arquivo anexado / Version of attached file:

Versão do Editor / Published Version

Mais informações no site da editora / Further information on publisher's website:

https://journals.aps.org/pra/abstract/10.1103/PhysRevA.95.062328

DOI: 10.1103/PhysRevA.95.062328

Direitos autorais / Publisher's copyright statement:

Long-time efficacy of the surface code in the presence of a super-Ohmic environment

D. A. López-Delgado,[1] E. Novais,[2] E. R. Mucciolo,[3] and A. O. Caldeira[1]

[1]*Departamento de Física da Matéria Condensada, Instituto de Física Gleb Wataghin,*
Universidade Estadual de Campinas, Campinas, São Paulo 13083-970, Brazil
[2]*Centro de Ciências Naturais e Humanas, Universidade Federal do ABC, Santo André, São Paulo 09210-170, Brazil*
[3]*Department of Physics, University of Central Florida, Orlando, Florida 32816, USA*
(Received 19 December 2016; published 23 June 2017)

We study the long-time evolution of a quantum memory coupled to a bosonic environment on which quantum error correction (QEC) is performed using the surface code. The memory's evolution encompasses N QEC cycles, each of them yielding a nonerror syndrome. This assumption makes our analysis independent of the recovery process. We map the expression for the time evolution of the memory onto the partition function of an equivalent statistical-mechanical spin system. In the super-Ohmic dissipation case the long-time evolution of the memory has the same behavior as the time evolution for just one QEC cycle. For this case we find analytical expressions for the critical parameters of the order-disorder phase transition of an equivalent spin system. These critical parameters determine the threshold value for the system-environment coupling below which it is possible to preserve the memory's state.

I. INTRODUCTION

It is widely accepted that large-scale quantum information processing will demand some sort of quantum error correction (QEC) as a fundamental part of its design [1–3]. The standard analysis of QEC codes deals with their efficiency against stochastic errors [4,5]. Although stochastic error models can sometimes be justified on physical grounds, often, they are used for their simplicity rather than their accuracy in describing the effect of realistic environments. Thus, it is important to complement these studies to include errors caused by environments that can be microscopically modeled [6–9]. In particular, Gaussian bosonic environments are amenable to analytical and numerical studies and have characteristics that are beyond the standard stochastic models, such as correlations and memory effects.

The surface code is regarded as a paradigmatic QEC code [1,10–14]. It requires only local gates and has a large "threshold" against stochastic error. In addition to the usual stochastic error threshold, it has also been partially benchmarked against Gaussian error models [8,15–18]. Unfortunately, all previous work focused only on the quantum information fidelity after a single QEC cycle.

In this paper, we take the discussion of the efficiency of the surface code against Gaussian noise one step forward. We provide analytical expressions for the logical qubit fidelity after an arbitrary number of QEC cycles in the presence of a bosonic Gaussian environment. We then specialize the calculation for a particular "super-Ohmic" environment and demonstrate that there are two possible regimes, depending on whether the coupling between the qubits and the environment is below or above a critical value: (i) below the critical value, information is preserved by QEC; (ii) information is lost otherwise. We further demonstrate that the "threshold" for a super-Ohmic environment is identical to the "threshold" for a single QEC cycle. Hence, we demonstrate that for a super-Ohmic environment memory effects and correlations between QEC cycles are unimportant, thus confirming an old conjecture for a dense set of qubits [19].

We start our discussion in Sec. II by describing all the assumptions built into our calculation. In Sec. III, we derive the analytical expression for the fidelity after many QEC cycles and specialize the calculation for a super-Ohmic environment in Sec. IV. Finally, we present our conclusions and perspectives in Sec. V.

II. THE SURFACE CODE IN A GAUSSIAN ENVIRONMENT

All threshold analyses of QEC are based on some assumptions about the system and its environment. We start by presenting all the assumptions built into our expressions for the logical qubit fidelity in a concise and itemized fashion to make the text clear and accessible. Our assumptions are, in general, favorable to the success of QEC. Therefore, our results must be regarded as an upper bound to the efficiency of the code against Gaussian noise. We follow the list of assumptions with a brief review of the surface code in Sec. II A and, finally, introduce the Gaussian bosonic environment in Sec. II B.

The following assumptions relate to the ability to manipulate qubits:

(i) In order to avoid additional assumptions about how quantum gates are performed [20], we focus on a quantum memory. In other words, after quantum information is encoded into the logical Hilbert space, no quantum gate is performed.

(ii) In a real situation, syndrome extraction would be faulty and time-consuming and could excite the environment [21]. Thus, some modeling of the measurement apparatus and quantum gates would have to be considered. In order to avoid this extra layer of complexity, we opt for considering the syndrome extraction to be flawless and instantaneous.

(iii) We assume that the initial logical state can be prepared flawlessly and it is disentangled from the environment. This is consistent with the previous assumption and its justification.

(iv) We derive a general expression for the fidelity of the logical qubit after several QEC steps. At the end of each cycle different syndromes could be measured, and a proper recovery operation would have to be performed [22]. In our calculation we bypass the discussion of a recovery strategy by

assuming that all syndrome measurements return a nonerror (more precisely, no detectable errors). Even though this is a very particular evolution, it is the only one that does not depend on a recovery strategy.

Many discussions of the threshold assume an optimal decoder, thus bypassing the need to discuss details in the recovery procedure. Unfortunately, in a correlated environment, the assumption of an optimal decoder does not completely solve the issue since an imprint of the particular syndrome remains in the environment and could potentially change the threshold. Among all possible syndromes, the nonerror syndrome is the one with the smallest imprint. Hence, our assumption of a nonerror syndrome must be understood as an upper limit to the surface code threshold in a correlated environment.

There are several possible microscopic models that apply to real environments. However, very few choices are amenable to an analytical or numerical calculation. In order to gain some insight into the basic structure of a quantum environment and its effects on the surface code threshold, we assume the following:

(i) The environment can be initially refrigerated to its lowest possible energy state. It is conceivable that over a long period of time an environment can be refrigerated to extremely low temperatures. This constitutes the very best scenario for quantum information processing since it provides the best possible coherence times. However, more likely in practice, after this initial step, the dynamics between the qubits and the environment can lead to excitations in the environment. We thus assume that the duration of the QEC is shorter than the time needed to refrigerate the environment.

(ii) In order to derive an exact analytical expression for the evolution operator of the qubits, we restrict the errors induced by the environment to bit flips.

(iii) There are many possible dispersion relations for a Gaussian environment. A particularly simple choice is to consider a linear dispersion relation, $\omega_k = v|\mathbf{k}|$, and a constant velocity of excitations v. This is not a restricting choice, just a convenient one. A more crucial quantity to be defined is the environment's spectral function [23–25].

(iv) It is natural to assume the existence of a large cutoff frequency for the environmental modes ω_Λ. Although the ultraviolet cutoff can be a large number, physical characteristics of the system and the environment make it finite. Typically, form factors in the coupling between the qubits and the environment define an ultraviolet scale to the system. A simple example is a charge qubit in a double quantum dot. The highest-frequency phonon that couples to this qubit is not of the order of the Debye frequency, but it is set by the inverse of the distance between the dots [26].

A. Surface code

The physical qubits in the surface code are arranged on the edges of a square lattice, forming themselves a square lattice slanted by $45°$. The QEC scheme is based on the stabilizer formalism [27] with two sets of stabilizers: plaquettes,

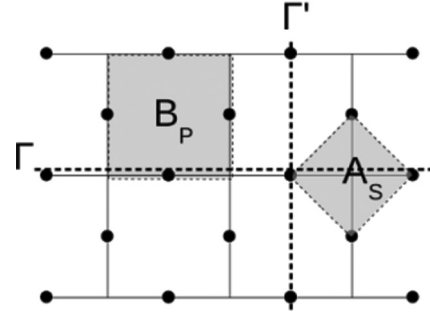$$B_P = \prod_{i \in P} \sigma_i^z, \tag{1}$$

FIG. 1. The surface code. Physical qubits are shown as black dots. The stabilizer operators are products of four Pauli operators, A_S and B_P. Logical operators correspond to a string of Pauli operators crossing the qubit lattice from one side to the other, Γ and Γ'.

and stars,

$$A_S = \prod_{i \in S} \sigma_i^x, \tag{2}$$

as shown in Fig. 1.

When all stabilizers are enforced, the lattice of physical qubits in Fig. 1 encodes one logical qubit. The logical bit-flip operator $\bar{X}$ is the product of physical bit-flip operators σ^x along a path from the upper to the lower sides of the lattice, e.g., through path Γ in Fig. 1. Similarly, a logical phase-flip operator $\bar{Z}$ is the product of physical phase-flip operators σ^z joining the vertical boundaries of the lattice, e.g., path Γ' in Fig. 1.

Additional logical qubits can be encoded in the same set of physical qubits by relaxing the stabilizers constraints [5]. However, the case of a single logical qubit is expected to have the largest possible threshold. Hence, we focus on this situation and define the logical states as

$$|\bar{\uparrow}\rangle = \frac{1}{\sqrt{N_\diamond}} G |F\rangle \tag{3}$$

and

$$|\bar{\downarrow}\rangle = \bar{X} |\bar{\uparrow}\rangle, \tag{4}$$

where $|F\rangle$ is the ferromagnetic z state of the physical qubits, $N_\diamond$ is a normalization constant, $G = \prod_\diamond (1 + A_\diamond)$, and $\prod_\diamond$ is the product over all star stabilizers.

B. Environment

The traditional "system-plus-environment" approach to open quantum systems [25,28] is the most natural method to systematically study memory effects and spatial correlations. In this approach, the environment is described by a large set of harmonic oscillators,

$$H_0 = \sum_{\mathbf{k}} \omega_{\mathbf{k}} a_{\mathbf{k}}^\dagger a_{\mathbf{k}}, \tag{5}$$

where $a_{\mathbf{k}}$ and $a_{\mathbf{k}}^\dagger$ are bosonic annihilation and creation operators that have the usual canonical commutation relations, i.e., $[a_{\mathbf{k}}, a_{\mathbf{k}'}^\dagger] = \delta_{\mathbf{k},\mathbf{k}'}$, where we set $\hbar = 1$. The environmental modes have momentum $k_i = \frac{2\pi}{L} n_i$, with n_i being an integer

and L being a macroscopic characteristic length. Finally, following our assumptions, we consider the dispersion relation, $\omega_\mathbf{k} = v|\mathbf{k}|$.

The full quantum evolution is given by the Hamiltonian

$$H = H_0 + V, \tag{6}$$

where V is the interaction between the qubits and the environment. It has the interaction Hamiltonian [24,29]

$$V = \lambda \sum_\mathbf{r} f(\mathbf{r})\sigma_\mathbf{r}^x, \tag{7}$$

where the Pauli operator $\sigma_\mathbf{r}^x$ acts on a physical qubit located at lattice position $\mathbf{r}$ and $f(\mathbf{r})$ is the bosonic operator,

$$f(\mathbf{r}) = \frac{(v/\omega_0)^{D/2+s}}{L^{D/2}} \sum_{\mathbf{k}\neq 0} |\mathbf{k}|^s (e^{+i\mathbf{k}\cdot\mathbf{r}}a_\mathbf{k}^\dagger + \text{H. c.}). \tag{8}$$

In Eq. (8), ω_0 is a characteristic microscopic frequency scale, and D is the number of spatial dimensions of the environment. The power s defines the low-frequency behavior of the environment's spectral density, as we show below. The coupling constants of all qubits with the environment are assumed to be identical.

A pure bit-flip error model does not constitute a full quantum error model [3]. Despite its limitations, in many physical systems there is a dominant decoherence channel. Hence, discussing the pure bit-flip error model is not an academic exercise. In addition, the model is amenable to an analytical treatment.

It is straightforward to derive the time-evolution operator in the interaction picture after a time Δ,

$$\hat{U}(\Delta,0) = T_t e^{-i\lambda \int_0^\Delta dt \sum_\mathbf{r} \hat{f}(\mathbf{r},t)\sigma_\mathbf{r}^x}, \tag{9}$$

where

$$\hat{f}(\mathbf{r},t) = \frac{1}{L^{D/2}} \sum_{\mathbf{k}\neq 0} |\mathbf{k}|^s (e^{+i\mathbf{k}\cdot\mathbf{r}+i\omega_k t}a_\mathbf{k}^\dagger + e^{-i\mathbf{k}\cdot\mathbf{r}-i\omega_k t}a_\mathbf{k}) \tag{10}$$

and T_t is the time-ordering operator.

Although the dispersion relation of the environment is an important quantity, what traditionally defines the type of environment is its spectral density,

$$J(\omega) \equiv \frac{\pi}{2} \sum_k \frac{C_k^2}{m_k \omega_k} \delta(\omega - \omega_k). \tag{11}$$

Here C_k comes from the interaction term, Eq. (7), when we consider qubits to be continuous-variable systems tunneling between the two degenerate minima of positions $\pm q_0$ in a bistable potential [24]. The coordinate of these systems is coupled to the ones of the bosons q_k (coordinate-coordinate coupling). In this scheme this interaction potential takes the form $V = q_0 \sigma_x \sum_k C_k q_k$, where the length scale q_0 is introduced in such a way we recover the appropriate dimension of the interaction term.

In order to identify C_k for our model, we use Eqs. (7) and (8), and $q_k = \sqrt{1/2m_k\omega_k}(a_k + a_k^\dagger)$. In this way we get

$$C_k^2 = 2\lambda^2 \frac{(v/\omega_0)^{D+2s}}{q_0^2 L^D} m_k v k^{2s+1}. \tag{12}$$

Now we can calculate the spectral density. We do this by inserting C_k^2 into Eq. (11) and taking the continuum limit (i.e., $\frac{(2\pi)^D}{L^D} \sum_k \to \int d^D k$). Finally, we assume a two-dimensional environment, i.e., $D = 2$, and perform the corresponding integration, obtaining

$$J(\omega) = \frac{2\lambda^2}{q_0^2 \omega_0^{2+2s}} \omega^{2s+1}. \tag{13}$$

Thus, following the standard definition, a two-dimensional environment with $s < 0$ is known as sub-Ohmic, while for $s = 0$ and $s > 0$ it is known as Ohmic and super-Ohmic, respectively.

We can use some of the properties of Gaussian environments to simplify Eq. (10) [18]. We first use the Magnus expansion [30] for the evolution operator to deal with the time-ordering operator and then normally order the exponentials, finally arriving at

$$\hat{U}(\Delta,0) = \left[\prod_{\mathbf{k}\neq 0} e^{-\hat{\mathcal{G}}(\mathbf{k},\Delta,0)} e^{-i\hat{\alpha}(\mathbf{k},\Delta,0)a_\mathbf{k}^\dagger} e^{-i\hat{\alpha}^*(\mathbf{k},\Delta,0)a_\mathbf{k}}\right], \tag{14}$$

where

$$\hat{\alpha}(\mathbf{k},\Delta,0) = \frac{\lambda}{L^{D/2}} \int_{\Delta(n-1)}^{\Delta n} dt \sum_\mathbf{r} |\mathbf{k}|^s \hat{\sigma}_{\mathbf{r},n}^x e^{+i\mathbf{k}\cdot\mathbf{r}+i\omega_k t} \tag{15}$$

and

$$\hat{\mathcal{G}}(\mathbf{k}) = -\frac{\lambda^2}{L^D}(v/\omega_0)^{D+2s} \int_0^\Delta dt_1 \int_0^\Delta dt_2 \theta(t_1 - t_2)$$
$$\times \sum_{\mathbf{r},\mathbf{r}'} |\mathbf{k}|^{2s} e^{-i\mathbf{k}\cdot(\mathbf{r}-\mathbf{r}')-i\omega_k(t_1-t_2)} \hat{\sigma}_\mathbf{r}^x \hat{\sigma}_{\mathbf{r}'}^x. \tag{16}$$

A detailed derivation of these steps can be found in Ref. [18].

For later convenience, we rewrite Eq. (14) in the qubit x basis $\{|\pm\rangle\}$, where $\hat{\sigma}^x|\pm\rangle = \pm|\pm\rangle$. By defining $|\bar{\sigma}\rangle$ as a configuration of qubits with eigenvalue $\sigma_\mathbf{r}^x = \pm 1$ for the qubit at position $\mathbf{r}$, we recast Eq. (14) as

$$\hat{U}(\Delta,0) = \sum_{\bar{\sigma}} u(\bar{\sigma})|\bar{\sigma}\rangle\langle\bar{\sigma}|, \tag{17}$$

where $\bar{\sigma} = \{\sigma_\mathbf{r}^x\}$ denotes the full set of spin variables, the pure bosonic operator is defined as

$$u(\bar{\sigma}) = \prod_{\mathbf{k}\neq 0} e^{-\mathcal{G}(\mathbf{k})} e^{-i\alpha(\mathbf{k})a_\mathbf{k}^\dagger} e^{-i\alpha^*(\mathbf{k})a_\mathbf{k}}, \tag{18}$$

and the auxiliary functions are given by

$$\mathcal{G}(\mathbf{k}) = -\frac{\lambda^2}{L^D}(v/\omega_0)^{D+2s} \int_0^\Delta dt_1 \int_0^\Delta dt_2 \theta(t_1 - t_2)$$
$$\times \sum_{\mathbf{r},\mathbf{r}'} |\mathbf{k}|^{2s} e^{-i\mathbf{k}\cdot(\mathbf{r}-\mathbf{r}')-i\omega_k(t_1-t_2)} \sigma_\mathbf{r}^x \sigma_{\mathbf{r}'}^x, \tag{19}$$

$$\alpha(\mathbf{k},\Delta,0) = \frac{\lambda}{L^{D/2}} \int_{\Delta(n-1)}^{\Delta n} dt \sum_\mathbf{r} |\mathbf{k}|^s \sigma_{\mathbf{r},n}^x e^{+i\mathbf{k}\cdot\mathbf{r}+i\omega_k t}. \tag{20}$$

III. LOGICAL QUBIT FIDELITY

We initially set the system in the logical state $|\bar{\uparrow}\rangle$ and assume that the environment is in its ground state $|0\rangle$,

$$|\psi_0\rangle = |\bar{\uparrow}\rangle \otimes |0\rangle. \tag{21}$$

We consider that the syndromes are extracted at equal time intervals of duration Δ and that the extraction is performed instantaneously. Hence, the full evolution operator is composed of a sequence of unitary evolutions and projections. In the simplest case of a nonerror syndrome, where there is no recovery operation to be performed, the quantum state after N cycles is given by

$$\begin{aligned}|\psi\rangle = \mathcal{P}_0\, U(N\Delta,(N-1)\Delta) \\ \cdots \mathcal{P}_0\, U(2\Delta,\Delta)\mathcal{P}_0\, U(\Delta,0)|\psi_0\rangle,\end{aligned} \tag{22}$$

where

$$\mathcal{P}_0 = |\bar{\uparrow}\rangle\langle\bar{\uparrow}| + \bar{X}|\bar{\uparrow}\rangle\langle\bar{\uparrow}|\bar{X}. \tag{23}$$

We now introduce a subscript to the spin-variable sets to designate the QEC step where the spin states evolve and use Eq. (17) to rewrite

$$\begin{aligned}|\psi\rangle = \sum_{\bar{\sigma}_1...\bar{\sigma}_N} [u(\bar{\sigma}_N)\cdots u(\bar{\sigma}_2)\, u(\bar{\sigma}_1)|0\rangle]\mathcal{P}_0|\bar{\sigma}_N\rangle \\ \times \langle\bar{\sigma}_N|\mathcal{P}_0|\bar{\sigma}_{N-1}\rangle \cdots \langle\bar{\sigma}_2|\mathcal{P}_0|\bar{\sigma}_1\rangle\langle\bar{\sigma}_1|\bar{\uparrow}\rangle,\end{aligned} \tag{24}$$

where $\sigma_{\mathbf{r}}^x|\bar{\sigma}_n\rangle = \sigma_{\mathbf{r},n}|\bar{\sigma}_n\rangle$ and $\sigma_{\mathbf{r},n} = \pm 1$. Since we have already integrated over time in Eqs. (19) and (20), these labels work now as new time variables.

The projectors can also be easily expressed in the x basis of the qubits,

$$\mathcal{P}_0 = \frac{1}{2^M N_\Diamond} \sum_{\bar{\sigma},\bar{\sigma}'} \sum_{\mathcal{J}=\{\bar{I},\bar{X}\}} G\mathcal{J}|\bar{\sigma}\rangle\langle\bar{\sigma}'|\mathcal{J}G, \tag{25}$$

where M is the total number of qubits and $\{\bar{\sigma},\bar{\sigma}'\}$ are two independent sums of all qubit configurations in the x basis. After relabeling the indices and using the property $G^2 = N_\Diamond G$, we obtain

$$\begin{aligned}|\psi\rangle = \frac{1}{\sqrt{\mathcal{N}}} \sum_{\{\bar{\sigma}_i,\mathcal{J}_i\}} \left[\prod_{n=0}^{N-1} u(\bar{\sigma}_n)|0\rangle\right] \\ \times \mathcal{J}_{N-1}\, G|\bar{\sigma}_{N-1}\rangle \prod_{n=0}^{N-2} \langle\bar{\sigma}_n|\mathcal{J}_n\, G|\bar{\sigma}_n\rangle,\end{aligned} \tag{26}$$

with $\mathcal{N}$ being a normalization constant and $\mathcal{J}_i = \{\bar{I},\bar{X}\}$.

When we use Eq. (26) to evaluate an expectation value, we have terms with the same "time" label coming from the ket and the bra. Hence, it is convenient to differentiate the origin of each term by renaming the variables in the bra $\langle\psi|$ as

$$\begin{aligned}\sigma &\to \tau, \\ \alpha &\to \beta, \\ \mathcal{J} &\to \mathcal{K}.\end{aligned}$$

It is now straightforward to write the logical state fidelity after N QEC cycles,

$$\mathcal{F} = \frac{\langle\psi|\bar{\uparrow}\rangle\langle\bar{\uparrow}|\psi\rangle}{\langle\psi|\psi\rangle}, \tag{27}$$

where

$$\langle\psi|\bar{\uparrow}\rangle\langle\bar{\uparrow}|\psi\rangle = \frac{1}{\mathcal{N}} \sum_{\{\bar{\sigma}_i,\bar{\tau}_i\}} {\sum_{\{\mathcal{J}_i,\mathcal{K}_i\}}}' \langle 0|\left[\prod_{k=N-1}^{0} u^\dagger(\bar{\tau}_k)\right]\left[\prod_{j=0}^{N-1} u(\bar{\sigma}_j)\right]|0\rangle \prod_{l=0}^{N-1} \langle\bar{\tau}_l|\mathcal{J}_l\, G|\bar{\tau}_l\rangle\langle\bar{\sigma}_l|\mathcal{J}_l\, G|\bar{\sigma}_l\rangle, \tag{28}$$

where $\sum'$ denotes a summation with the restrictions $\mathcal{J}_0 = \mathcal{K}_0 = \mathcal{J}_{N-1} = \mathcal{K}_{N-1} = \bar{I}$. Similarly,

$$\langle\psi|\psi\rangle = \frac{1}{\mathcal{N}} \sum_{\{\bar{\sigma}_i,\bar{\tau}_i\}} \sum_{\{\mathcal{J}_i,\mathcal{K}_i\}} \langle 0|\left[\prod_{k=N-1}^{0} u^\dagger(\bar{\tau}_k)\right]\left[\prod_{j=0}^{N-1} u(\bar{\sigma}_j)\right]|0\rangle \prod_{l=0}^{N-1} \langle\bar{\tau}_l|\mathcal{J}_l\, G|\bar{\tau}_l\rangle\langle\bar{\sigma}_l|\mathcal{J}_l\, G|\bar{\sigma}_l\rangle, \tag{29}$$

but with no restrictions on $\mathcal{J}_n$ or $\mathcal{K}_n$. Notice $\langle\psi|\psi\rangle \neq 0$ in general since the time evolution of the system is nonunitary.

To further simplify these expressions, we normally order the expectation value of the bosonic operators. This is a tedious task but is easily performed using the Baker-Campbell-Hausdorff formula. For instance,

$$e^{-i\alpha^*(\mathbf{k},n)\, a_\mathbf{k}}\, e^{-i\alpha(\mathbf{k},m)\, a_\mathbf{k}^\dagger} = e^{-i\alpha(\mathbf{k},m)\, a_\mathbf{k}^\dagger}\, e^{-i\alpha^*(\mathbf{k},n)\, a_\mathbf{k}} e^{-\alpha^*(\mathbf{k},n)\, \alpha(\mathbf{k},m)}. \tag{30}$$

After performing several commutations to normally order the bosonic operators, we obtain

$$\begin{aligned}\langle 0|\left[\prod_{k=N-1}^{0} u^\dagger(\bar{\tau}_k)\right]\left[\prod_{j=0}^{N-1} u(\bar{\sigma}_j)\right]|0\rangle = \prod_{\mathbf{k}\neq 0} &\exp\left\{-\sum_{n=0}^{N-1}[\mathcal{G}(\mathbf{k},n) + \mathcal{G}^*(\mathbf{k},n) - \beta^*(\mathbf{k},n)\, \alpha(\mathbf{k},n)]\right\} \\ &\times \exp\left\{-\sum_{n=1}^{N-1}\sum_{m=0}^{n-1}[\alpha^*(\mathbf{k},n)\, \alpha(\mathbf{k},m) + \beta(\mathbf{k},n)\, \beta^*(\mathbf{k},m)\right. \\ &\qquad\qquad \left. - \beta^*(\mathbf{k},n)\, \alpha(\mathbf{k},m) - \alpha(\mathbf{k},n)\, \beta^*(\mathbf{k},m)]\right\}.\end{aligned} \tag{31}$$

It is natural to rewrite this equation in the short and suggestive form of an exponential,

$$\langle 0| \left[\prod_{k=N-1}^{0} u^\dagger(\bar{\tau}_k) \right] \left[\prod_{j=0}^{N-1} u(\bar{\sigma}_j) \right] |0\rangle = e^{-\mathcal{H}}, \tag{32}$$

where

$$\mathcal{H} = \sum_{\mathbf{r},\mathbf{s}} \Bigg\{ \sum_{n=0}^{N-1} F_1(\mathbf{r}-\mathbf{s},0)\,(\tau_{\mathbf{r},n}-\sigma_{\mathbf{r},n})(\tau_{\mathbf{s},n}-\sigma_{\mathbf{s},n}) + i\,\Phi_1(\mathbf{r}-\mathbf{s})\,(\tau_{\mathbf{s},n}-\sigma_{\mathbf{s},n})(\tau_{\mathbf{r},n}+\sigma_{\mathbf{r},n}) + i\,\Phi_2(\mathbf{r}-\mathbf{s},0)(\tau_{\mathbf{s},n}\sigma_{\mathbf{r},n}-\tau_{\mathbf{r},n}\sigma_{\mathbf{s},n})$$

$$- \sum_{n=1}^{N-1}\sum_{m=0}^{n-1} [F_1(\mathbf{r}-\mathbf{s},n-m)-\Phi_3(\mathbf{r}-\mathbf{s},n-m)](\tau_{\mathbf{r},n}-\sigma_{\mathbf{r},n})(\tau_{\mathbf{s},m}-\sigma_{\mathbf{s},m}) + i\,[F_2(\mathbf{r}-\mathbf{s},n-m)$$

$$+ \Phi_3(\mathbf{r}-\mathbf{s},n-m)]\,(\tau_{\mathbf{r},n}-\sigma_{\mathbf{r},n})(\tau_{\mathbf{s},m}+\sigma_{\mathbf{s},m}) \Bigg\} \tag{33}$$

and

$$F_1(\mathbf{r},n) = \frac{\lambda^2 (v/\omega_0)^{D+2s}}{L^D} \sum_{\mathbf{k}\neq 0} |\mathbf{k}|^{2s} \left[\frac{1-\cos(\omega_k\Delta)}{\omega_k^2} \right] \cos(\mathbf{k}\cdot\mathbf{r})\cos(n\omega_k\Delta), \tag{34a}$$

$$F_2(\mathbf{r},n) = \frac{\lambda^2 (v/\omega_0)^{D+2s}}{L^D} \sum_{\mathbf{k}\neq 0} |\mathbf{k}|^{2s} \left[\frac{1-\cos(\omega_k\Delta)}{\omega_k^2} \right] \cos(\mathbf{k}\cdot\mathbf{r})\sin(n\omega_k\Delta), \tag{34b}$$

$$\Phi_1(\mathbf{r},n) = \frac{\lambda^2 (v/\omega_0)^{D+2s}}{L^D} \sum_{\mathbf{k}\neq 0} |\mathbf{k}|^{2s} \left[\frac{\omega_k\Delta-\sin(\omega_k\Delta)}{\omega_k^2} \right] \cos(\mathbf{k}\cdot\mathbf{r}), \tag{34c}$$

$$\Phi_2(\mathbf{r},n) = \frac{\lambda^2 (v/\omega_0)^{D+2s}}{L^D} \sum_{\mathbf{k}\neq 0} |\mathbf{k}|^{2s} \left[\frac{1-\cos(\omega_k\Delta)}{\omega_k^2} \right] \sin(\mathbf{k}\cdot\mathbf{r})\cos(n\omega_k\Delta), \tag{34d}$$

$$\Phi_3(\mathbf{r},n) = \frac{\lambda^2 (v/\omega_0)^{D+2s}}{L^D} \sum_{\mathbf{k}\neq 0} |\mathbf{k}|^{2s} \left[\frac{1-\cos(\omega_k\Delta)}{\omega_k^2} \right] \sin(\mathbf{k}\cdot\mathbf{r})\sin(n\omega_k\Delta). \tag{34e}$$

Equation (33) can be interpreted as a statistical-mechanics Hamiltonian of a three-dimensional lattice of Ising variables with uniform interactions. The three dimensions are due to the two-dimensional spatial lattice of the qubits and the discrete "time" direction. The different correlation functions originating from the bosonic model produce interactions between these Ising variables that can be long or short ranged.

Using this notation, the logical qubit fidelity can be cast as

$$\mathcal{F} = \frac{\sum'_{\bar{\sigma},\bar{\tau}} e^{-\mathcal{H}} \prod_l \langle \bar{\tau}_l| \mathcal{J}_l\, G |\bar{\tau}_l\rangle \langle \bar{\sigma}_l| \mathcal{J}_l\, G |\bar{\sigma}_l\rangle}{\sum_{\bar{\sigma},\bar{\tau}} e^{-\mathcal{H}} \prod_l \langle \bar{\tau}_l| \mathcal{J}_l\, G |\bar{\tau}_l\rangle \langle \bar{\sigma}_l| \mathcal{J}_l\, G |\bar{\sigma}_l\rangle}. \tag{35}$$

There are two aspects to consider when analyzing this expression. First, the sum over the Ising variables in the numerator is constrained to the positive stars due to the projector G. Hence, not all Ising configurations of the three-dimensional lattice contribute to the sums. Second, the "energy cost" imposed by $\mathcal{H}$ assigns different weights to the terms of the sum. Because of exchange symmetry $\sigma \leftrightarrow \tau$, these contributions are always real (but very difficult to evaluate).

It is possible to numerically study Eq. (35). For small lattices a "brute-force", exact approach is viable. Some insight can be gained with these simulations, but in order to determine the threshold, large lattices are needed. The most obvious option is to use a Monte Carlo algorithm to evaluate the fidelity.

Unfortunately, the oscillating (imaginary) terms present in Eqs. (34) hinders this approach. The long-range nature of the interactions also make the convergence of any Monte Carlo–based method very slow.

In Sec. IV we evaluate the fidelity for a particular set of environment parameters that allow for an analytical solution.

IV. SUPER-OHMIC ENVIRONMENT WITH $s = 1/2$

A very interesting case to consider has $s = 1/2$ and $D = 2$. This corresponds to a super-Ohmic environment where analytical expressions for the correlation functions in Eqs. (34) can be easily written by imposing the continuum limit [15]

$$\frac{(2\pi)^2}{L^2} \sum_{\mathbf{k}} \rightarrow \int_0^\Lambda \rho\, d\rho \int_0^{2\pi} d\theta.$$

As usual when dealing with super-Ohmic environments, some values for the variables $\mathbf{r}$ and n in Eqs. (34) can lead to ultraviolet diverging contributions. The leading divergent terms are linearly proportional to the ultraviolet cutoff,

$$F_1(0,0) \approx \frac{\lambda^2 v \Lambda}{2\pi \omega_0^3} \tag{36}$$

and

$$F_1(0,1) \approx -\frac{\lambda^2 v}{2\pi \omega_0^3} \frac{\Lambda}{2}, \tag{37}$$

with the remaining terms giving subleading contributions diverging with the cutoff or no divergence at all. Hence, for a large environmental cutoff, in leading order, it is a good approximation to simplify Eq. (33) to

$$\mathcal{H} \approx \frac{J}{4} \sum_{n=0}^{N-1} \sum_{\mathbf{r}} \Big[(\tau_{\mathbf{r},n} - \sigma_{\mathbf{r},n})(\tau_{\mathbf{r},n} - \sigma_{\mathbf{r},n}) \tag{38}$$

$$+ \frac{1}{2}(\tau_{\mathbf{r},n} - \sigma_{\mathbf{r},n})(\tau_{\mathbf{r},n+1} - \sigma_{\mathbf{r},n+1})\Big], \tag{39}$$

where $J = \frac{2\lambda^2 v}{\pi \omega_0^3}\Lambda$.

We can now introduce the spin-1 operator

$$S_{\mathbf{r},n} \equiv \frac{1}{2}(\tau_{\mathbf{r},n} - \sigma_{\mathbf{r},n}) \tag{40}$$

and write

$$\mathcal{H} \approx J \sum_{n=0}^{N-1} \sum_{\mathbf{r}} \left(S_{\mathbf{r},n}^2 + \frac{1}{2} S_{\mathbf{r},n} S_{\mathbf{r},n+1} \right), \tag{41}$$

which can be interpreted as the Hamiltonian of decoupled spin-1 chains along the "time" direction of the statistical-mechanics model associated with the fidelity calculation.

The first term in Eq. (41), $S_{\mathbf{r},n}^2$, is a "zero-field splitting" (also known as on-site anisotropy) and competes with the exchange coupling $S_{\mathbf{r},n} S_{\mathbf{r},n+1}$. The physics of this statistical-mechanical model is well known [31], and for the numerical prefactors on the right-hand side of Eq. (41) there are no phase transitions and no magnetic ordering. This means that the qubit configurations between QEC cycles do not energetically constrain each other in the calculation evaluating the fidelity through Eq. (35). Hence, we can find the threshold by discussing the critical coupling in a single QEC cycle. This result provides a more rigorous justification for the usual assumption that for a super-Ohmic environment memory and correlations induced by the environment can be neglected in the evaluation of the threshold.

The fidelity can be evaluated as

$$\mathcal{F} = \frac{\sum'_{\bar{\sigma},\bar{\tau}} \prod_l e^{-\mathcal{H}_l} \langle \bar{\tau}_l | \mathcal{J}_l \, G | \bar{\tau}_l \rangle \langle \bar{\sigma}_l | \mathcal{J}_l \, G | \bar{\sigma}_l \rangle}{\sum_{\bar{\sigma},\bar{\tau}} \prod_l e^{-\mathcal{H}_l} \langle \bar{\tau}_l | \mathcal{J}_l \, G | \bar{\tau}_l \rangle \langle \bar{\sigma}_l | \mathcal{J}_l \, G | \bar{\sigma}_l \rangle}, \tag{42}$$

where the single-chain Hamiltonian is given by

$$\mathcal{H}_l = J S_{\mathbf{r},l}^2. \tag{43}$$

Although there is no explicit interaction between the spin-1 variables, the constraint of positive stars make the evaluation of the fidelity nontrivial. The simplest method to deal with the constraint is to use "mass-field variables" [16,18]. The mass field μ is an Ising variable defined in the center of each plaquette. The variable $\sigma_{\mathbf{r}}$ in the link between two plaquettes is written as the product of the mass field of each plaquette. For example, for bulk sites in Fig. 2,

$$\sigma_{\mathbf{r},l} = \mu_{\mathbf{x},l} \, \mu_{\mathbf{y},l} \tag{44}$$

and

$$\tau_{\mathbf{r},l} = \nu_{\mathbf{x},l} \, \nu_{\mathbf{y},l}. \tag{45}$$
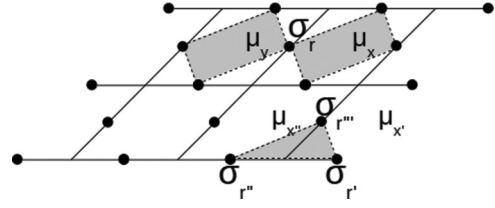

FIG. 2. Illustration of mass field variables in the bulk and in the boundary for the spin variable σ.

We can now replace the sum over the constrained σ and τ variables with an unconstrained sum over the μ and ν variables.

The only issue remaining is the top and bottom lattice boundaries. Stars located at the boundary are formed by only three qubits, but because of the positive-star constraint the mass-field variables at these boundaries always assume the same value [16],

$$\mu_{\mathbf{p}',l} \, \sigma_{\mathbf{r}',l} = \mu_{\mathbf{p}'',l} \, \sigma_{\mathbf{r}'',l} := \alpha_l = \pm 1 \tag{46}$$

and

$$\nu_{\mathbf{p}',l} \, \tau_{\mathbf{r}',l} = \nu_{\mathbf{p}'',l} \, \tau_{\mathbf{r}'',l} := \beta_l = \pm 1. \tag{47}$$

Using the new variables, Eq. (43) can be rewritten as

$$\mathcal{H}_l = -\frac{J}{4} \left(\sum_{\langle \mathbf{p},\mathbf{p}' \rangle \in \text{bulk}} \nu_{\mathbf{p},l} \, \nu_{\mathbf{p}',l} \, \mu_{\mathbf{p},l} \, \mu_{\mathbf{p}',l} \right.$$
$$\left. + \sum_{\mathbf{p} \in \text{boundary}} \alpha_{\mathbf{p},l} \, \nu_{\mathbf{p},l} \, \mu_{\mathbf{p},l} \right), \tag{48}$$

with no restrictions on the values of the mass-field variables. We can further simplify the problem by noticing that the change of variables

$$s_{\mathbf{p},l} = \nu_{\mathbf{p},l} \, \mu_{\mathbf{p},l} \tag{49}$$

maps Eq. (48) into a square-lattice Ising model with boundary fields [18]

$$\mathcal{H}_l = -\frac{J}{4} \left(\sum_{\langle \mathbf{p},\mathbf{p}' \rangle \in \text{bulk}} s_{\mathbf{p},l} \, s_{\mathbf{p}',l} + \alpha_l \, \beta_l \sum_{\mathbf{p} \in \text{boundary}} s_{\mathbf{p},l} \right). \tag{50}$$

Following our previous work on this model and on the surface code fidelity calculation [16,18] and using the Onsager solution [32], we know that this model has a second-order phase transition at the critical coupling

$$J_c = 2\ln(1 + \sqrt{2}). \tag{51}$$

Thus, for $J > J_c$ the Ising model is in its ordered phase, and the fidelity is smaller than unity. Conversely, for $J < J_c$ the Ising model is in its paramagnetic phase, and the fidelity is unity [16,18]. Thus, the critical coupling constant for the surface code in this super-Ohmic environment is

$$\lambda_c \approx 2\sqrt{\frac{\pi \omega_0^3}{v\Lambda} \ln(1 + \sqrt{2})}. \tag{52}$$

V. SUMMARY AND CONCLUSIONS

There is a large body of theoretical work in which the efficiency of QEC is analyzed. One of the most common methods employed is the use of the operator norm for the interaction Hamiltonian. However, this method is not applicable to models with diverging norms, such as the spin boson [33–35]. An alternative method is to use a master equation for the quantum evolution of the reduced density matrix ρ_r [29]. Even though the master equation formalism is very general, some very stringent assumptions must be made even in the simplest cases in order to obtain workable expressions. In addition, the initial step of the formalism is to integrate the environmental degrees of freedom. Hence, it explicitly precludes any correlations induced by the environment between qubits at different QEC steps. In this paper we followed a third route: the Feynman-Vernon influence functional formalism [29].

We followed the full quantum evolution of the system and the environment, and only at the end of the QEC evolution did we trace the environment. For a single QEC step, both the influence functional formalism and a well-performed Lindblad description are expected to yield similar results. However, due to the syndrome extraction procedure, this equivalence may not hold when many QEC cycles are considered.

For a pure bit-flip model, it was possible to write the exact time-evolution operator and then obtain an exact closed form for a logical qubit fidelity after an arbitrary number of QEC cycles, Eq. (35). Even for this simple pure bit-flip model the expression is daunting. For the surface code it corresponds to a three-dimensional lattice of interacting Ising variables that are constrained by the nature of the QEC code. This result can be understood in terms of a fictitious statistical-mechanical problem [6,20]. In this language, the QEC threshold corresponds to a "phase transition", where the system-environment coupling is mapped onto an effective inverse temperature. For a very small coupling (corresponding to a high-temperature phase) the statistical-mechanical problem is in its disorder phase, and QEC is able to keep the fidelity equal to unity. However, for large couplings (corresponding to a low-temperature phase) the qubits can "order", and the fidelity becomes smaller than unity.

We specialized the calculation for the super-Ohmic case with $s = 1/2$ and a two-dimensional environment. Super-Ohmic environments are plagued with ultraviolet divergencies in some of the correlation functions that yield interactions between qubits. In the particular example of $s = 1/2$ the leading diverging terms have a linear dependence on the ultraviolet cutoff. Although we performed an explicit calculation for this particular value of s, similar results also hold for any $s > 0$ case. Therefore, the discussion in Sec. IV can be extended for all super-Ohmic cases.

In Sec. IV we demonstrated that the statistical-mechanical problem defined by Eq. (35) can be simplified in the super-Ohmic case to an array of spin-1 chains, Eq. (41). The particular set of parameters that emerged from the calculation tells us that the array is in a phase where the zero-field-splitting term is dominant. Hence, the model can be further simplified, and only this zero-field-splitting term needs to be kept. This analysis justifies the use of stochastic error models in the discussion of the QEC threshold for super-Ohmic environments. The model has an analytical solution, allowing us to find an expression for the critical coupling where the threshold takes place, Eq. (52).

In summary, we provided an exact expression for the fidelity of a logical qubit in the surface code in the presence of a bosonic environment after an arbitrary number of QEC steps. We demonstrated that for super-Ohmic environments the use of stochastic models is fully justifiable, thus confirming with an explicit example an old conjecture in the literature [19].

[1] D. P. DiVincenzo, Phys. Scr. **T137**, 014020 (2009).

[2] G. Waldherr, Y. Wang, S. Zaiser, M. Jamali, T. Schulte-Herbrüggen, H. Abe, T. Ohshima, J. Isoya, J. F. Du, P. Neumann, and J. Wrachtrup, Nature (London) **506**, 204 (2014).

[3] *Quantum Error Correction*, edited by D. A. Lidar and T. A. Brun (Cambridge University Press, Cambridge, 2013).

[4] S. Bravyi, M. B. Hastings, and S. Michalakis, J. Math. Phys. **51**, 093512 (2010).

[5] A. G. Fowler, M. Mariantoni, J. M. Martinis, and A. N. Cleland, Phys. Rev. A **86**, 032324 (2012).

[6] E. Novais, E. R. Mucciolo, and H. U. Baranger, Phys. Rev. Lett. **98**, 040501 (2007).

[7] H. K. Ng and J. Preskill, Phys. Rev. A **79**, 032318 (2009).

[8] E. Novais and E. R. Mucciolo, Phys. Rev. Lett. **110**, 010502 (2013).

[9] J. Preskill, Quantum Inf. Comput. **13**, 0181 (2013).

[10] S. B. Bravyi and A. Y. Kitaev, arXiv:quant-ph/9811052.

[11] E. Dennis, A. Kitaev, A. Landahl, and J. Preskill, J. Math. Phys. **43**, 4452 (2002).

[12] A. G. Fowler, A. M. Stephens, and P. Groszkowski, Phys. Rev. A **80**, 052312 (2009).

[13] P. Sarvepalli and R. Raussendorf, in *Theory of Quantum Computation, Communication, and Cryptography*, edited by W. VanDam, V. M. Kendon, and S. Severini, Lecture Notes in Computer Science Vol. 6519 (Springer-Verlag, Berlin, Heidelberg, 2011), pp. 47–62.

[14] A. G. Fowler, A. C. Whiteside, and L. C. L. Hollenberg, Phys. Rev. Lett. **108**, 180501 (2012).

[15] P. Jouzdani, E. Novais, and E. R. Mucciolo, Phys. Rev. A **88**, 012336 (2013).

[16] P. Jouzdani, E. Novais, I. S. Tupitsyn, and E. R. Mucciolo, Phys. Rev. A **90**, 042315 (2014).

[17] C. G. Brell, S. Burton, G. Dauphinais, S. T. Flammia, and D. Poulin, Phys. Rev. X **4**, 031058 (2014).

[18] E. Novais, A. Stanforth, and E. R. Mucciolo, Phys. Rev. A **95**, 042339 (2017).

[19] E. Novais, E. R. Mucciolo, and H. U. Baranger, Phys. Rev. A **82**, 020303 (2010).

[20] E. Novais, E. R. Mucciolo, and H. U. Baranger, Phys. Rev. A **78**, 012314 (2008).

[21] D. P. DiVincenzo and P. Aliferis, Phys. Rev. Lett. **98**, 020501 (2007).

[22] G. Duclos-Cianci and D. Poulin, Phys. Rev. Lett. **104**, 050504 (2010).

[23] A. O. Caldeira and A. J. Leggett, Ann. Phys. (NY) **149**, 374 (1983).

[24] H. Breuer and F. Petruccione, *The Theory of Open Quantum Systems* (Oxford University Press, Oxford, 2007).

[25] A. O. Caldeira, *An Introduction to Macroscopic Quantum Phenomena and Quantum Dissipation* (Cambridge University Press, Cambridge, 2014).

[26] S. Vorojtsov, E. R. Mucciolo, and H. U. Baranger, Phys. Rev. B **71**, 205322 (2005).

[27] M. A. Nielsen and I. L. Chuang, *Quantum Computation and Quantum Information* (Cambridge University Press, Cambridge, 2000).

[28] A. J. Leggett, S. Chakravarty, A. T. Dorsey, M. P. A. Fisher, A. Garg, and W. Zwerger, Rev. Mod. Phys. **59**, 1 (1987).

[29] S. Weiss, *Quantum Dissipative Systems*, 2nd ed. (World Scientific, Cambridge, 1999).

[30] S. Blanes, F. Casas, J. Oteo, and J. Ros, Phys. Rep. **470**, 151 (2009).

[31] H. W. Capel, Physica **32**, 966 (1966).

[32] L. Onsager, Phys. Rev. **65**, 117 (1944).

[33] B. M. Terhal and G. Burkard, Phys. Rev. A **71**, 012336 (2005).

[34] P. Aliferis, D. Gottesman, and J. Preskill, Quantum Inf. Comput. **6**, 97 (2006).

[35] D. Aharonov, A. Kitaev, and J. Preskill, Phys. Rev. Lett. **96**, 050504 (2006).